Electronic Supplementary Material (ESI) for Lab on a Chip.

Supplementary information

Intestinal Explant Barrier Chip: long-term intestinal absorption screening in a novel microphysiological system using tissue explants

Hossein Eslami Amirabadi[1,2,7], Joanne M. Donkers[1,7], Esmée Wierenga[1], Bastiaan Ingenhut[3], Lisanne Pieters[1], Lianne Stevens[1,4], Tim Donkers[5], Joost Westerhout[6], Rosalinde Masereeuw[2], Ivana Bobeldijk-Pastorova[1], Irene Nooijen[1], Evita van de Steeg[1]

[1]Department of Metabolic Health Research, the Netherlands Organization for Applied Scientific Research (TNO), Zeist, the Netherlands. [2]Division of Pharmacology, Utrecht Institute for Pharmaceutical Sciences, Utrecht University, Utrecht, the Netherlands. [3]Materials solution department, TNO, and Brightlands Materials Centre, Geleen, the Netherlands. [4]Department of Surgery, Division of Transplantation, Leiden University Medical Centre, Leiden, the Netherlands. [5]Division of Space systems engineering, TNO, Delft, the Netherlands. [6]RAPID, TNO, Utrecht, the Netherlands. [7]These authors contributed equally: Hossein Eslami Amirabadi, Joanne M. Donkers. *e-mail: evita.vandesteeg@tno.nl

Supplementary Experimental

Glucose and lactate measurements Glucose (D-glucose) and lactate (L-lactate) were measured in complete Williams E medium and in the apical and basolateral supernatants of the two-compartmental model using a glucose (K-GLUHK-110A, Megazyme) and lactate (K-LATE, Megazyme) assay kit according to the manufacturer's protocol. Absorbance (340 nm) was measured using the BioTek Synergy HT microplate reader (BioTek Instruments Inc., Winooski, VT).

Supplementary Tables

Table s1 | Mechanical properties of 9 specimens from the material used in the IEBC.

# Specimen	Elastic modulus (MPa)	Yield Strength (MPa)
1	3938.90	37.07
2	3465.63	32.20
3	3946.76	34.47
4	3680.60	34.61
5	3606.00	29.55
6	3863.52	24.20
7	3704.42	34.78
8	3577.31	30.79
9	3790.04	33.13

The elastic modulus and yield strength of the specimens were measured in a tensile test.

Table s2 | Recovery of test drugs in the IEBC with porcine tissue between 20-24 h

Test compound	t=20-24 hours (%)	Intracellular (%)
Mannitol	96.9 ± 1.4	1.0 ± 0.5
Metformin	95.0 ± 1.3	0.7 ± 0.6
Warfarin	93.7 ± 1.3	n.d.
Caffeine	93.3 ± 1.2	n.d.
Acyclovir	93.3 ± 1.5	0.8 ± 0.5
Atenolol	93.3 ± 0.7	n.d.
Antipyrine	92.6 ± 1.6	n.d.

Compounds were ranked based on their recovery. Apical medium with radiolabeled test compounds (^{14}C for warfarin, metformin, acyclovir, antipyrine, caffeine or ^{3}H for atenolol, mannitol) and basolateral medium were refreshed at t = 20 h and radioactivity in the apical and basolateral compartments was measured at t = 24 h. To calculate the drug recovery, total radioactivity at t=24 h was compared to the refreshment dose at t = 20 h. The intracellular radioactivity indicates the percentage of radioactivity found in the tissue at t=24 h compared to the initial dose. Data are represented as mean ± SEM (warfarin, metformin, acyclovir: n=6-7 from 2 independent experiments; antipyrine, atenolol: n=9 from 3 independent experiments; caffeine and mannitol: n=15 from 4 independent experiments).

Supplementary Figures

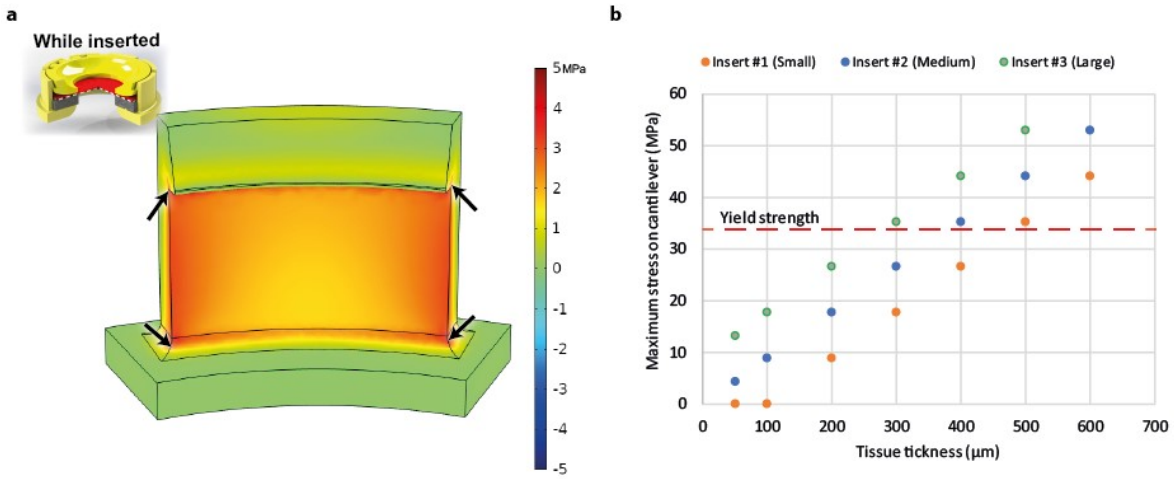

Fig. s1 | **Maximum stress on clicking walls when the tissue explant is fixed in the IEBC. a,** COMSOL Multiphysics simulation of a single cantilever when the tissue explant is fixed in the snap fit mechanism. The color contour shows the von Mises stress on the cantilever when the rubber under the tissue is 0.1 mm compressed. The arrows show the locations of the maximum stress on the cantilever. **b**, Maximum stress on the cantilever as a function of the thickness of the compressed tissue explant (under the fixing insert). Inserts with different thicknesses were used for tissues from different donors. Insert #2 is designed so that it deforms the rubber with the same value as the thickness of the tissue. For thinner and thicker tissue explants, thicker (#3) and thinner (#1) inserts were used, respectively. The difference between the thickness of the inserts was 100 µm. The dashed line shows the yield strength of the material (32.31 MPa).

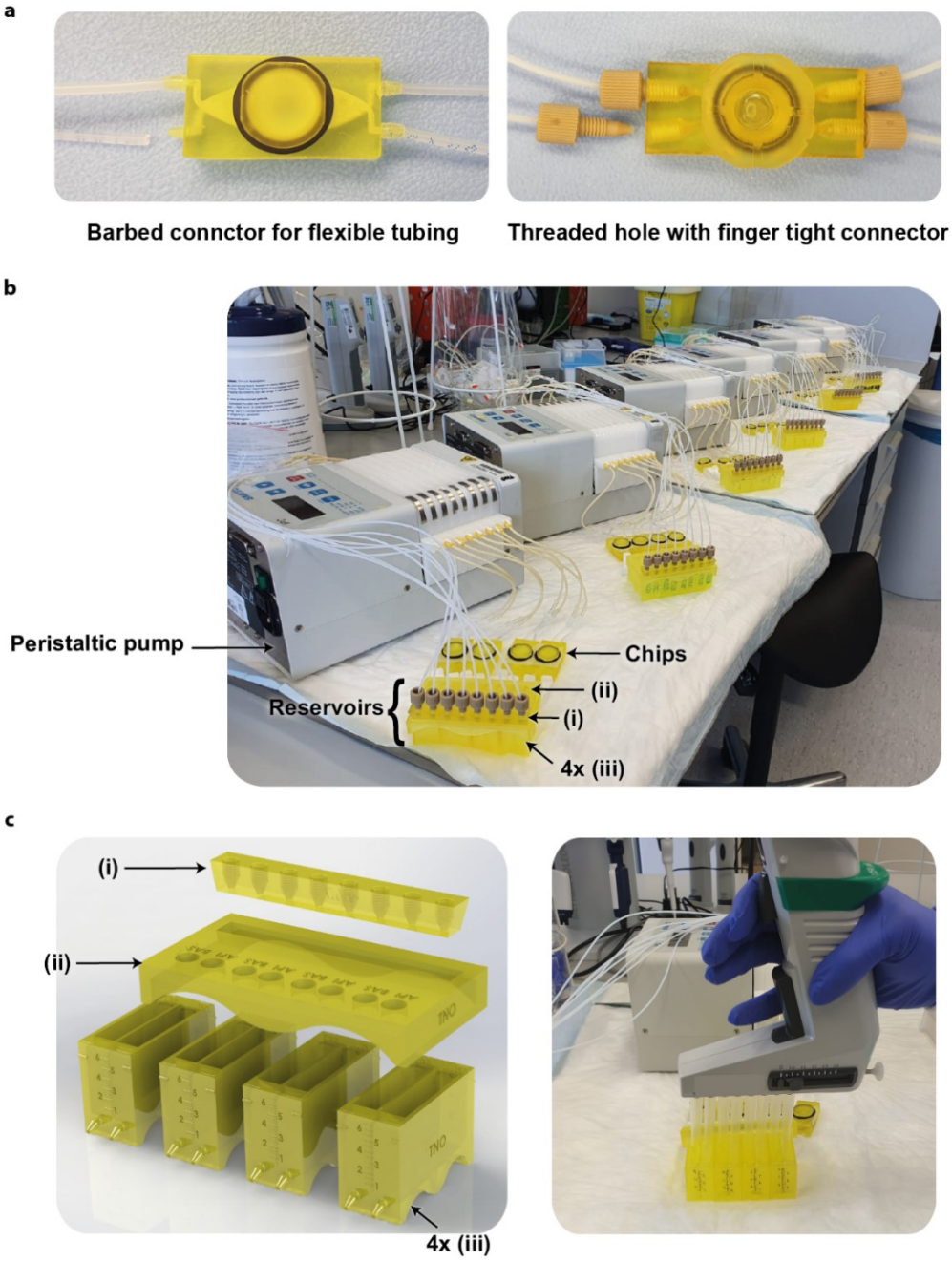

Fig. s2 | **An overview of the Explant Barrier Chip (EBC) system. a**, Standard 3D printed connections on the EBC. The images show barbed connectors and threaded holes suitable for finger tight connections. All the dimensions were adopted according to available standards. **b**, EBC microfluidic recirculation system. All media were added to the reservoirs. The peristaltic pump created a negative pressure and withdrew the media from the reservoirs through the chip and recirculated them back to the reservoirs. The tissue explant was placed between two microchannels which represented the apical and basolateral sides in the intestine. (i) is where the tubing from the pump connects to the reservoirs with standard connectors (sampling bar), (ii) is the lid of the reservoirs and (iii) is the reservoirs. **c**, Schematic exploded view and back view of assembled 3D printed reservoirs. (i), (ii) and (iii) are defined in **b**. The apical and basolateral reservoirs for each chip were printed in one block and four pairs of reservoirs, corresponding to four chips, were assembled under one lid. The reservoirs were connected to the chips via their standard connections at the bottom. The distance between the reservoirs were designed to follow the layout of a 96 wells plate, so multichannel pipettes can be used for applying media or sampling from top of the reservoirs.

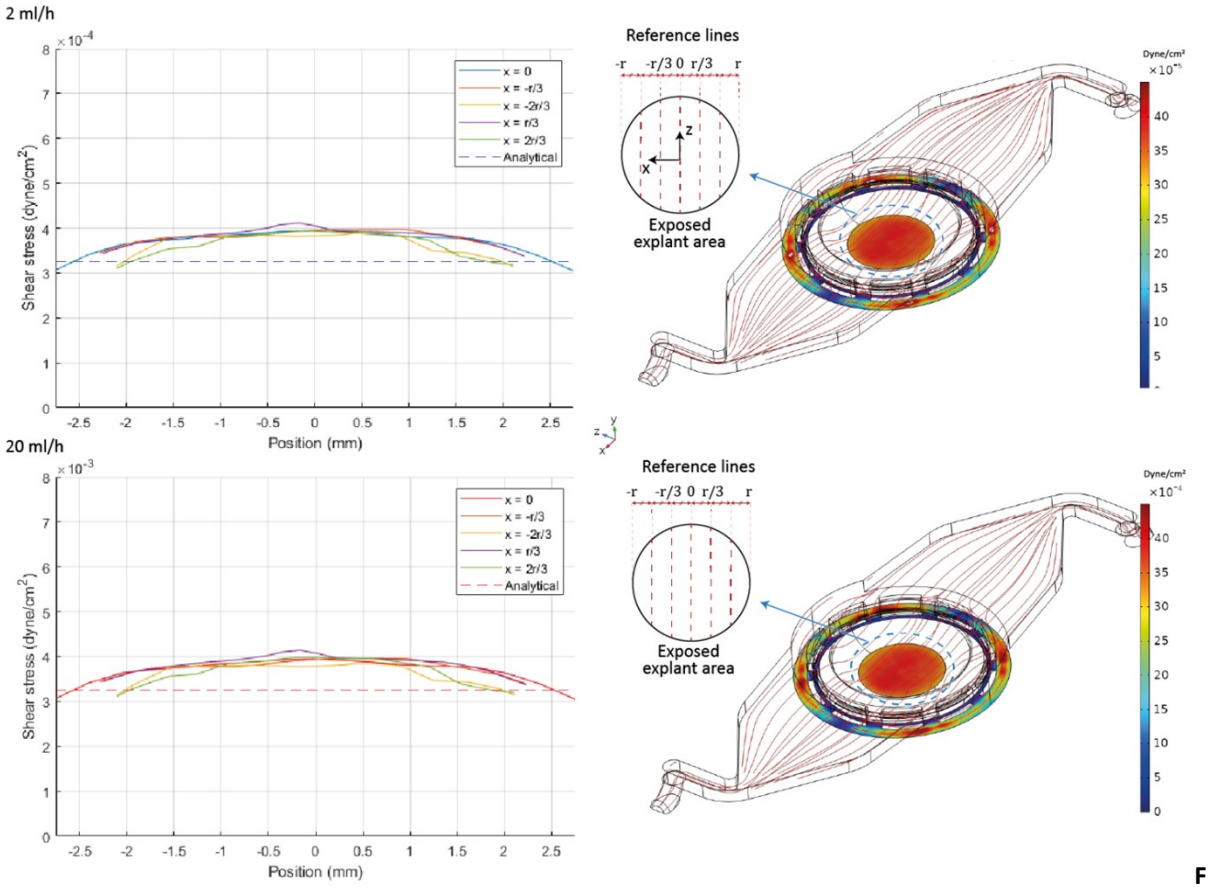

F

ig. s3 | **Shear stress distribution on the tissue explant at different flow rates.** COMSOL Multiphysics simulations were performed on the apical channel of the IEBC at 2 mL/h and 20 mL/h. The x-axis of the graphs show the position along the z-axis of the geometry on the right. Different lines in the graphs correspond to the reference lines with different x coordinates. For the analytical values, shear stress was derived from the parabolic velocity profile of a laminar flow on the bottom of a rectangular channel with the same height and width of the apical channel where the tissue explant is placed.

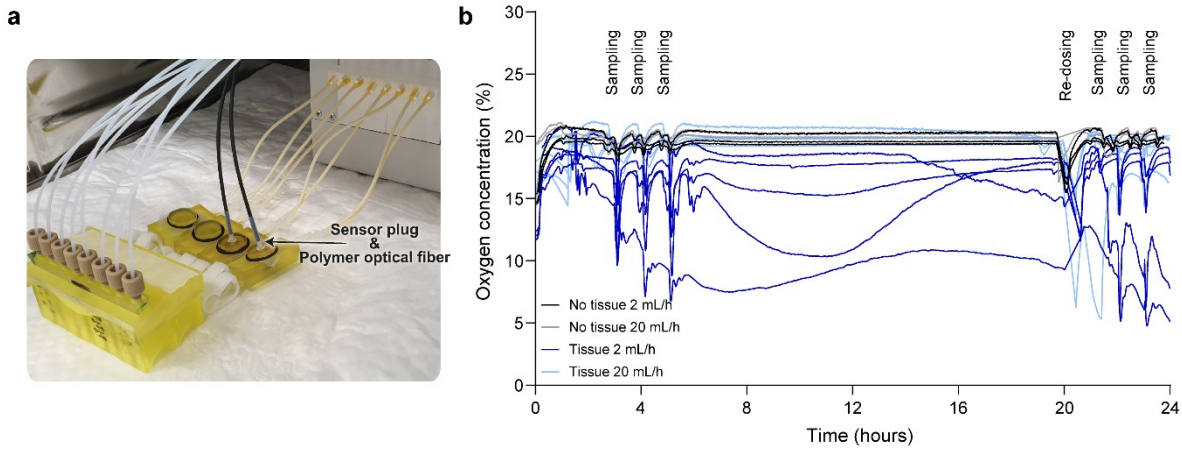

Fig. s4 | **Oxygen concentration in the IEBC, individual chips. a,** The IEBC set up with oxygen sensor plugs and optical fibers connected to the apical microchannel through the cap of the chip. The optical fibers are connected to an oxygen reader outside the incubator. **b,** Oxygen concentration in the apical medium on top of porcine colon tissue explants fixed in the IEBC or empty chips (without tissue) exposed to a flow rate of 2 or 20 mL/h for 24 hours. Oxygen concentrations were measured with one minute intervals, data represents the individual chips (n=5 for IEBC with tissue, n=2-3 for IEBC without tissue).

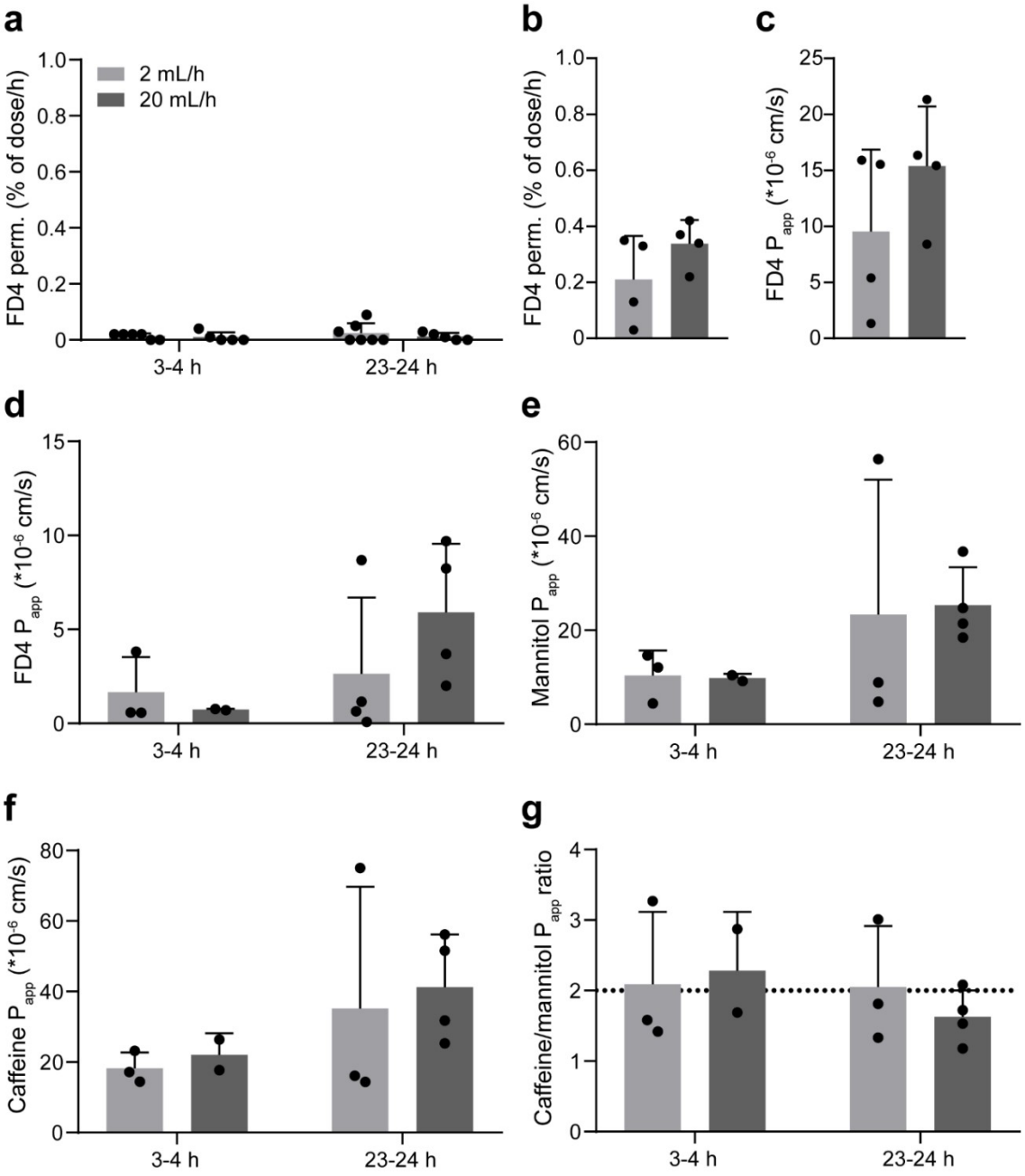

Fig. s5 | **FD4 permeability and caffeine and mannitol transport in the IEBC. a,** FITC-dextran-4000 Da (FD4, 50 µM) permeability (%/h) in human colon tissue explants, mounted in the IEBC and exposed to a flow rate of 2 or 20 mL/h for 24 hours. Tissue explants that showed good tissue integrity, <1%/h FD4 permeability, were included in subsequent data analysis (n=5-7/group, data collected from 4 independent experiments). **b-c**, FD4 permeability (%/h) **(b)** and apparent permeability (P_{app}) **(c)** of IEBC without tissue explants, exposed to a flow rate of 2 or 20 mL/h for 24 hours. Permeability and P_{app} were determined between 3-4, 4-5, 5-20, 20-22, 22-23, and 23-24 hours and were averaged (n=4 chips per condition). **d-g**, Human colon tissue explants were mounted in the IEBC and exposed to a flow rate of 2 or 20 mL/h for 24 hours (n=3-4/group). P_{app} of FD4 (50 µM) (**d**), mannitol (10 µM) (**e**), and caffeine (10 µM) (**f**) were determined between 3-4 hours and 23-24 hours. **g,** Ratio of transcellular transport (P_{app} caffeine) over paracellular transport (P_{app} mannitol). Dotted line indicates a P_{app} ratio of 2. Data are presented as mean + SEM (**a**) or mean + SD (**b-g**).

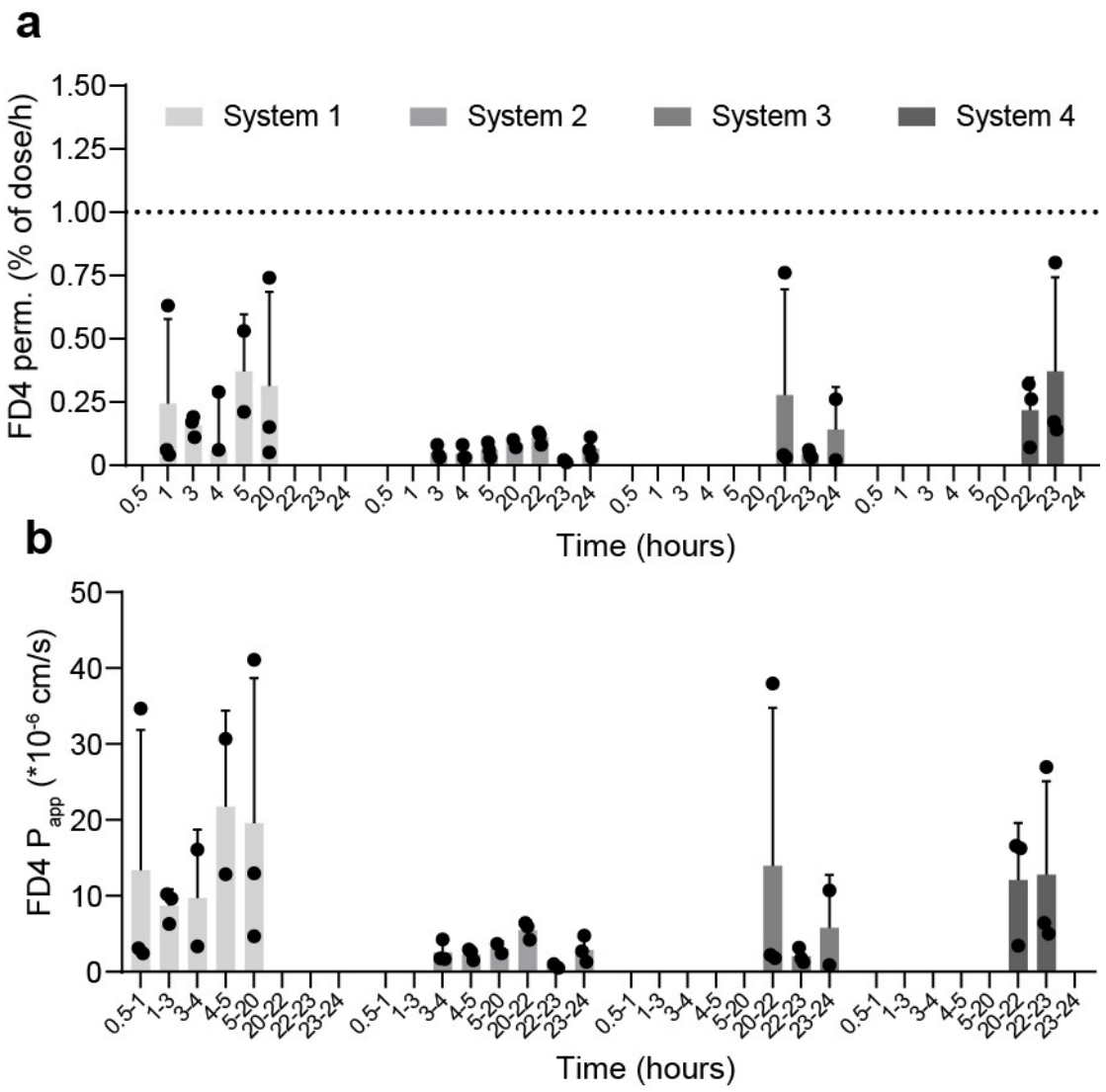

Fig. s6| **Impact of timing of compound administration on FD4 permeability and LDH secretion**. **a-d,** Porcine colon tissue explants were mounted in the IEBC and exposed to a flow rate of 2 mL/h for 24 hours (n=4/system). **a,** FD4 (50 µM) permeability (%/h) and **b,** P_{app} were determined at multiple time points. Data are presented as mean + SD.

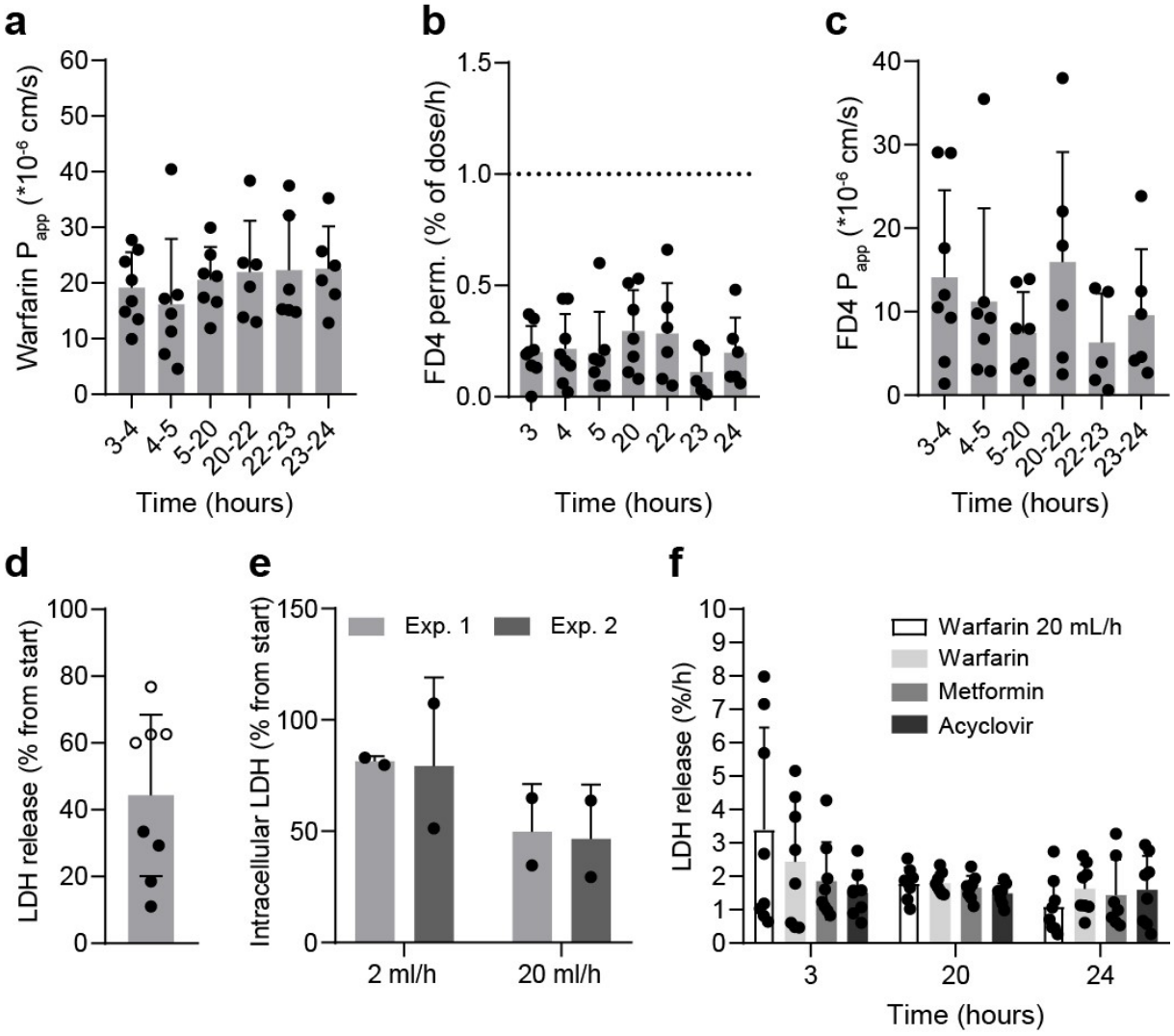

Fig. s7| **Permeability of warfarin and intracellular LDH levels in the IEBC. a-e,** Porcine colon tissue explants were mounted in the IEBC and exposed to a flow rate of 20 mL/h for 24 hours (n=8, data collected from 2 independent experiments). Warfarin (100 µM) P_{app} (**a**) and FD4 (50 µM) permeability (%/h) (**b**) and Papp (**c**) were determined at multiple time points. Dotted line in panel (**b**) indicates the cut off value of 1%/h. **d,** Cumulative LDH release into the apical and basolateral compartments was determined after 24 hours and compared to the level of intracellular LDH at t=0. **e,** Intracellular LDH levels (n=2/flow rate/experiment) from porcine colon tissue explants (panel a-d this figure and warfarin condition Fig. 6) were determined after 24 hours and compared to the level of intracellular LDH at t=0. **f,** Sum of apical and basolateral LDH release (%/h) at 3, 20 and 24 hours of incubation. The amount of secreted LDH was compared to the level of intracellular LDH at t=0. Data are presented as mean + SD.

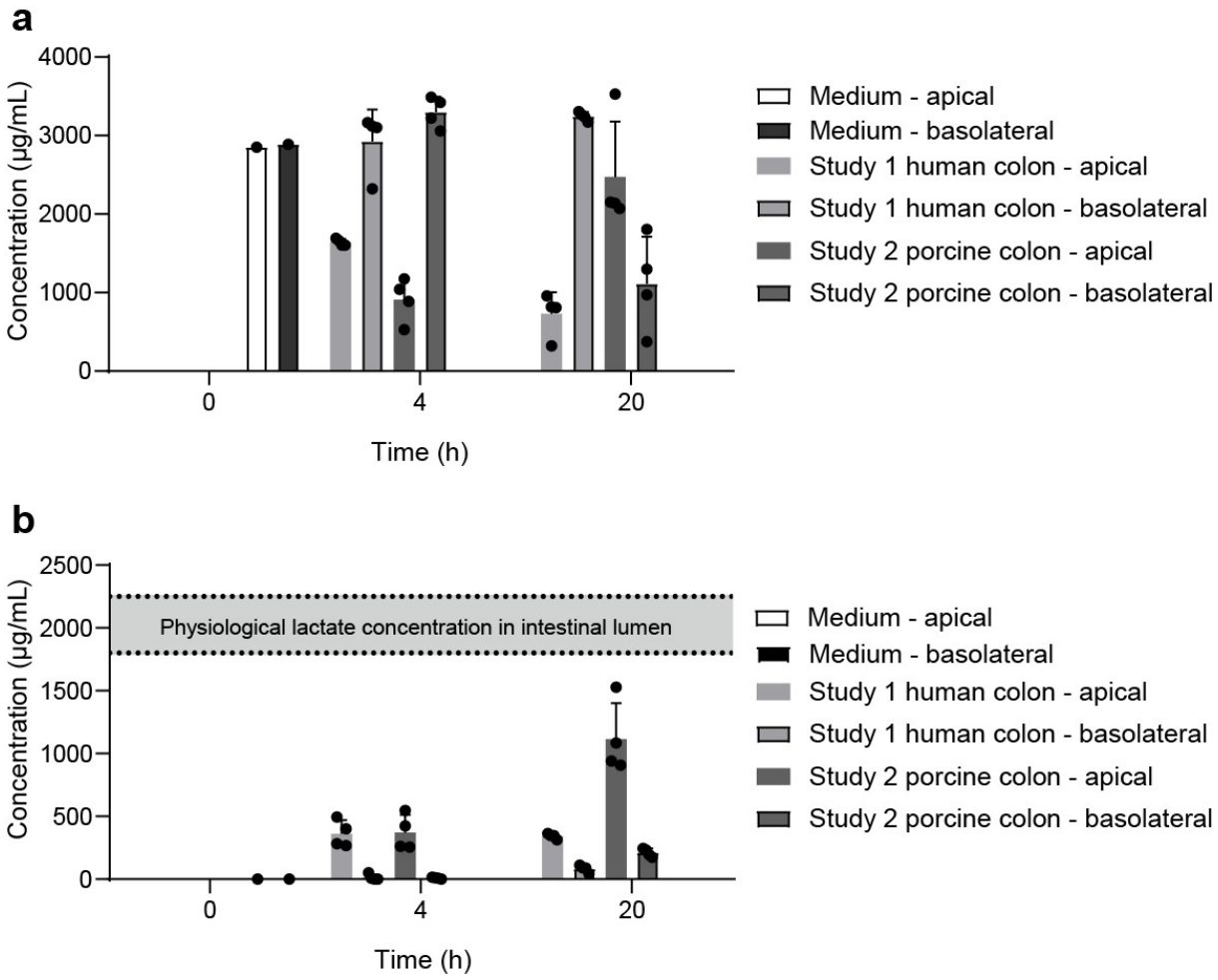

Fig. s8| Glucose and lactate concentrations in the apical and basolateral media. a-b, Glucose and lactate concentrations were determined in unexposed medium and in 4- or 20-hour exposed medium to human colon (study 1) or porcine colon (study 2) tissue explants in the IEBC (n=4/study). Apical and basolateral medium were collected and measured separately. **a,** Glucose concentration. **b,** Lactate concentration. Physiological lactate concentration in intestinal lumen[1] is indicated between the dotted lines. Data are presented as mean + SD.

Supplementary References

1 S. Kahlert, S. Junnikkala, L. Renner, U. Hynönen, R. Hartig, C. Nossol, A. Barta-Böszörményi, S. Dänicke, W. B. Souffrant, A. Palva, H. J. Rothkötter and J. Kluess, *PLoS One*, 2016, **11**, 1–17.